Bioelectrochemistry 78 (2010) 124–129

Contents lists available at ScienceDirect

Bioelectrochemistry

journal homepage: www.elsevier.com/locate/bioelechem

Carbon nanotube–hydroxyapatite–hemoglobin nanocomposites with high bioelectrocatalytic activity

H.Y. Zhao [a], X.X. Xu [a], J.X. Zhang [a], W. Zheng [a,*], Y.F. Zheng [a,b]

[a] Center for Biomedical Materials and Engineering, Harbin Engineering University, Harbin 150001, China
[b] Department of Advanced Materials and Nanotechnology, College of Engineering, Peking University, Beijing 100871, China

ARTICLE INFO

Article history:
Received 20 June 2009
Received in revised form 28 August 2009
Accepted 29 August 2009
Available online 6 September 2009

Keywords:
MWCNTs–HA
Hemoglobin
Direct electron transfer
Bioelectrochemistry
Electrocatalysis

ABSTRACT

In this paper, carbon nanotubes–hydroxyapatite (MWCNTs–HA) composite were synthesized by self-assembling technique, and investigated by X-ray diffraction, scanning electron microscopy (SEM) and FT-IR spectroscopy. Hemoglobin (Hb) immobilized in MWCNTs–HA film not only retained its similarly native conformations, but also achieved the direct electron transfer. The apparent heterogeneous electron transfer rate constant (k_s) was evaluated as $(5.05 \pm 0.41)\ s^{-1}$ according to Laviron's equation, and the surface coverage (Γ^*) was estimated as $(9.25 \pm 0.69) \times 10^{-10}$ mol cm^{-2}. Moreover, the Hb immobilized in MWCNTs–HA film exhibited remarkable bioelectrocatalytic activity for the electrochemical reduction of H_2O_2. The amperometric response of the biosensor varied linearly with the H_2O_2 concentration ranging from 0.5 μM to 2 μM, and the results showed a detection limit of 0.09 μM. Furthermore, the Hb-immobilized MWCNTs–HA film exhibited the excellent catalytic reactivity toward trichloroacetic acid (TCA).

1. Introduction

The study of the direct electron transfer between enzymes or proteins and electrodes has received considerable attention in recent years [1–7]. Because the studies on direct electron process between enzymes or proteins and electrodes cannot only provide us the information to elucidate their metabolic processes in the biological system, but also establish a foundation for constructing the third generation of electrochemical biosensors and a new kind of bioreactors. Hemoglobin (Hb), consisting of four subunits of polypeptide which contain four active centers, is an important protein in red blood cells, and in the reduced form, is the carrier of oxygen [8]. It is an ideal model molecule for the study of electron transfer reactions of heme proteins and also for biosensing and electrocatalysis [9–12]. However, it is difficult for Hb to exchange electron directly with the electrode surface due to the fact that the inaccessibility of its electroactive center and loss of electrochemical activities might occur when Hb was adsorbed directly on the electrode surface [1]. Therefore, in recent years, researchers make efforts to find appropriate matrix with good biocompatibility in order to improve the direct electron transfer [9–18].

Since the discovery of carbon nanotubes (CNTs) in 1991, the exceptional physicochemical properties of carbon nanotubes (CNTs), such as their unique structural, electrical, mechanical, electro-mechanical and physical properties, have made them emerge as an essential platform in nanoscience [19]. The direct electron communication between the redox sites of protein or enzyme and the electrode could be promoted by CNTs due to the three-dimensional configuration constructed by the dispersed CNTs on the electrode. Hence, CNTs become an attractive material in bioelectrochemistry for the direct electrochemistry of enzymes. However, the poor dissolution and biocompatibility of the CNTs limited the development of new designs of electrochemical sensors and biosensors. In order to overcome the difficulty, functionalization of CNTs has become the hotspot of improving the dispersion [20–22].

Hydroxyapatite (HA, $Ca_{10}(PO_4)_6(OH)_2$) with characteristic features of a biomaterial, in particular, a crystallographic similarity with natural bone minerals, can be derived from both synthetic and natural origins [23]. In this context, we proposed to fabricate a composite of HA-associated MWCNTs by the self-assembly method via an aqueous solution reaction. On the one hand, the associate HA is desirable for the improvement of the bioactivity and biocompatibility of composite [24,25]. On the other hand, suitable surface modification for MWCNTs can prevent themselves from aggregation and provide nucleation sites for HA. Moreover, the direct electron transfer and bioelectrocatalysis of the Hb co-assembled onto MWCNT–HA nanocomposite film were realized.

2. Experimental

2.1. Materials and apparatus

Multi-wall carbon nanotubes (MWCNTs, diameter 10–30 nm, length 1–50 μm) were purchased from Shenzhen Nanotech Port Co., Ltd (Shenzhen, China). Calcium chloride and disodium hydrogen

* Corresponding author. Center for Biomedical Materials and Engineering, Harbin Engineering University, No.145, Na-Tong-Da Street, Nan-Gang District, Harbin 150001, China. Tel./fax: +86 451 82518644.
E-mail address: zhengwei75@126.com (W. Zheng).

1567-5394/$ – see front matter © 2009 Elsevier B.V. All rights reserved.
doi:10.1016/j.bioelechem.2009.08.009

phosphate were provided by the Tianjin Chemical company. Bovine hemoglobin (Hb, MW 67,000) purchased from Sigma Chemical Co. was used without further purification. The hydrogen peroxide (30% (w/w)) and trichloroacetic acid were ordered from Beijing Chemical Company (Beijing, China).The dilute solution of H_2O_2 was prepared daily. Potassium dihydrogen orthophosphate (0.10 M) was used to prepare the supporting electrolyte and its pH value was adjusted to 7.0 using potassium hydroxide. Aqueous solutions were prepared using doubly distilled water. All other chemicals were of analytical grade and used without further purification.

XRD patterns of the crystals were obtained from a Shimadzu Lad-X 600 X-ray diffractometer using Cu K_α radiation. SEM images were obtained from MX2600FE (Camscan Company, Britain). FT-IR spectra were obtained on a Perkin-Elmer Spectrome 100 spectrometer (Perkin-Elmer Company, USA) at room temperature. UV–visible (UV–vis) absorption was carried out by using a 2550 spectrophotometer (Shimadzu, Japan).

Electrochemical measurements were carried out on a computer-controlled electrochemical analyzer (CHI 650C, CHI, Austin, TX) in a two-compartment and three-electrode cell containing 20 mL 0.10 M phosphate buffer (pH 7.0), which was used as the supporting electrolyte except that the pH-dependent experiments were carried out in phosphate buffer with various pH values. The modified GC electrodes were used as working electrodes, a platinum spiral wire and a saturated calomel electrode (SCE) as auxiliary and reference electrodes, respectively. For the experiments conducted under anaerobic condition, the electrolyte was bubbled with pure N_2 gas for more than 30 min and N_2 gas was kept flowing over the solution during the electrochemical measurements. All electrochemical measurements were performed at ambient temperature (18 ± 2 °C).

2.2. Synthesis of HA functionalized multi-walled carbon nanotubes (MWCNTs–HA) and preparation of the modified electrodes

MWCNTs in 3 mol L^{-1} nitric acid were sonicated for 20 min, then refluxed for 12 h at 90 °C in order to obtain the carboxyl functional group (MWCNTs–COOH). Then the mixture was filtered under vacuum through 0.45 μm millipore polycarbonate membrane and washed with distilled water until the pH value of the filtrate became 7. The resulting MWCNTs–COOH was dried under vacuum for 24 h at 100 °C. The MWCNTs–HA composite were prepared according to the literature with some modification [26]. Typically, 20 mg of MWCNTs–COOH was reacted with 5 ml of 0.02 mol L^{-1} aqueous solution of calcium chloride and strongly stirred for 1 h. To this mixture, 5 ml of 0.02 mol L^{-1} aqueous solution of disodium hydrogen phosphate was added dropwise with continuous stirring for 1 h. The product formed was filtered and washed several times with distilled water to remove any unreacted reagents and byproducts. Finally, the product was dried under vacuum for 24 h at 50 °C.

The bare glassy carbon (GC, 3 mm-diameter) was firstly polished before use with emery paper (# 2000), 0.3 and 0.05 μm alumina slurry on a woolen cloth, and then cleaned under bath sonication for

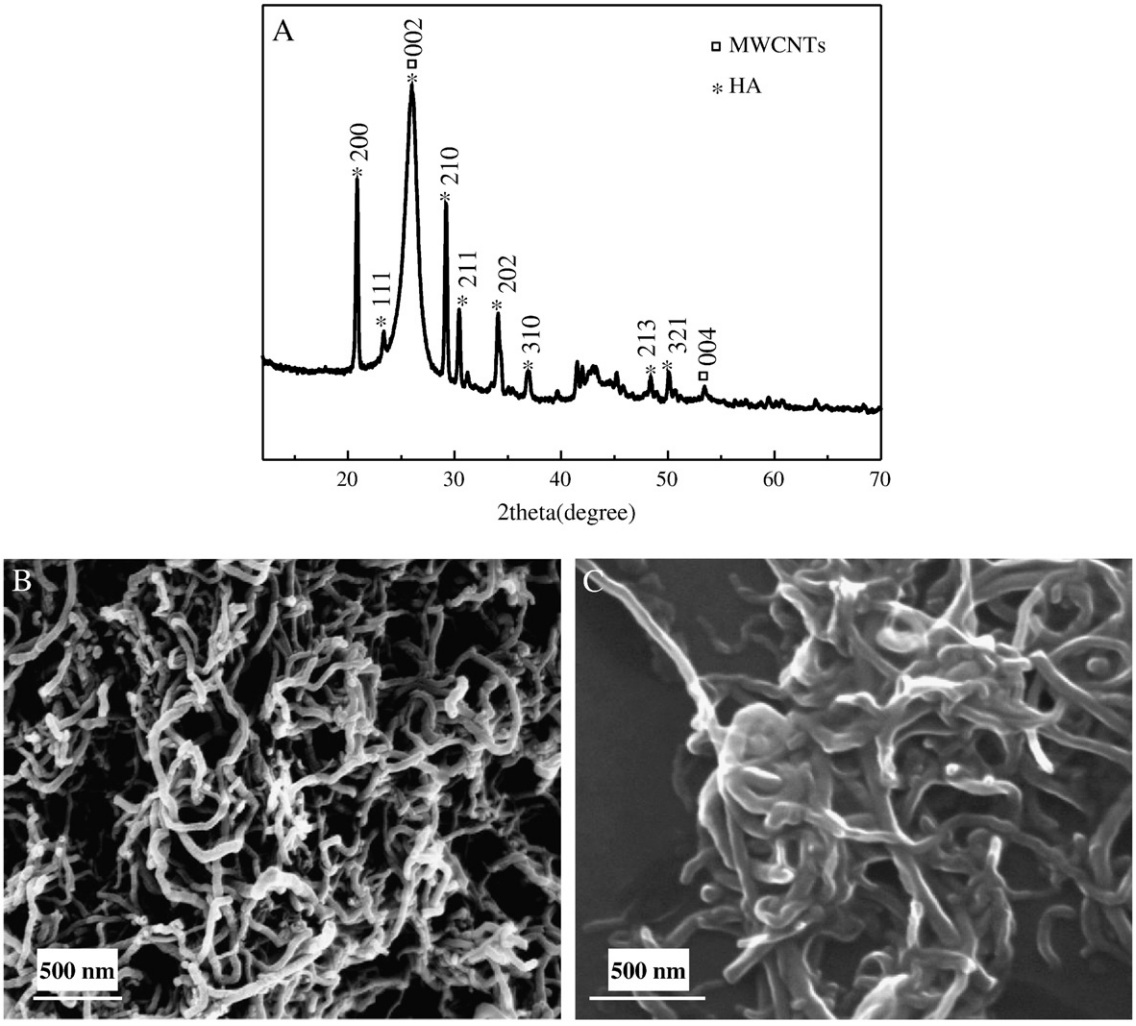

Fig. 1. XRD pattern(A), SEM image of MWCNTs–HA composite (B) and SEM image of pristine MWCNTs (C).

10 min and finally rinsed thoroughly with distilled water. The MWCNTs–HA (2 mg) was mixed in aqueous solution and was sonicated for 1 h at room temperature to obtain a homogeneous and black dispersion containing 2.0 mg mL^{-1} MWCNTs–HA. For the preparation of Hb/MWCNTs–HA/GC electrodes, a 4 μL of the dispersion was dip-coated onto the pretreated GC electrodes, followed by a period of standing in air until dry. Then the MWCNTs–HA/GC electrodes were immersed into 0.10 M phosphate buffer containing 20 mg mL^{-1} Hb for 48 h. The resulting electrodes (Hb/MWCNTs–HA/GC) were rinsed with distilled water prior to electrochemical measurements.

3. Results and discussion

3.1. Characterization of MWCNTs–HA nanocomposite

Fig. 1A illustrates the XRD patterns of the synthesized MWCNTs–HA nanocomposite powders. The peak positions are matching closely with the diffraction of synthesized HA (JCPD card number: 34-0010). In addition, the main diffraction peak at 26.0° for the MWCNTs attributing to the hexagonal graphite (002) planes was consistent with (002) planes of HA. Moreover, no peaks corresponding to $Ca_3(PO_4)_2$ appeared in Fig. 1A.

Fig. 1B and C display the typical SEM images of MWCNTs–HA nanocomposite and pristine MWCNTs. As can be seen from Fig. 1B, the surface of MWCNTs was not smooth, and appeared to be covered by a few mineral-substance. Moreover, compared with the pristine MWCNTs without any functionalization (Fig. 1C), the MWCNTs–HA nanocomposite could be well dispersed because the assembled HA would destroy the van der Waals interaction between carbon nanotubes. At the same time, as one of the most ideal biocompatible materials, HA might endow MWCNTs–HA nanocomposite an enhanced biocompatibility.

The formation of MWCNTs–HA nanocomposite was identified with FT-IR spectroscopy as show in Fig. 2A. For purified MWCNTs, the weak band at 1732 cm^{-1} corresponds to carbonyl (C=O) group indicating the presence of carboxylic group on the surface of MWCNTs [27]. Bands around 2923 cm^{-1} and 2854 cm^{-1} are due to asymmetric and symmetric stretching of C—H bonds [28]. As can be seen from the spectrum of MWCNTs–HA in Fig. 2A, the characteristic absorption peaks of phosphate group for HA were observed at 601 cm^{-1} and 728 cm^{-1}, 1034 cm^{-1}, 1108 cm^{-1}, which were attributed to ν_4 P—O bending, ν_2 OPO bending, and ν_3 asymmetrical of P—O stretching, respectively [29,30]. Moreover, the characteristic absorption bands at 3431 cm^{-1} of hydroxyl group for HA were also observed in the spectrum of the MWCNTs–HA nanocomposite. These results indicated the formation of HA on the MWCNTs matrix.

3.2. Conformational studies of Hb immobilized into MWCNTs–HA composite film

The amide I band in the region of 1600–1700 cm^{-1} is caused by C O stretching vibrations of peptide linkages in the backbone of protein and the amide II band in the region 1500–1600 cm^{-1} is caused by the combination of N–H in plane bending and C–N stretching vibrations of the peptide groups. The positions of the both amide bands can provide information about secondary structure of polypeptide chain because their positions are more sensitive to protein peptide chain conformational change [31]. As shown in Fig. 2A, the absorption bands at 1653 cm^{-1} and 1542 cm^{-1} for native Hb were observed, while after immobilized on the MWCNTs–HA film, the bands of amide I and amide II bands of Hb were found at 1653 cm^{-1} and 1548 cm^{-1}, which were the same as those of the native Hb. The results indicated that the MWCNTs–HA film might provide a promising matrix for enzyme immobilization and biosensor fabrication because of its excellent biocompatibility.

The UV–vis spectroscopy was carried out to investigate the conformational variations of Hb immobilized into the MWCNTs–HA films since UV–vis absorption spectroscopy can give structural information about the environmental surrounding of the heme prosthetic group of Hb [32]. The composite film contained MWCNTs–HA, Hb and Hb/MWCNTs–HA films were exhibited in Fig. 2B. As can be seen, the Hb entrapped in the MWCNTs–HA film has a characteristic Soret absorption at 413 nm, shifting only two nanometers compared with the native Hb for the Soret band of 411 nm. It indicated that the Hb entrapped in the MWCNTs–HA composite films could retain its native structure because of the good biocompatibility of the MWCNTs–HA composite films.

3.3. Direct electrochemistry of Hb/MWCNTs–HA composite film

The direct electrochemistry behavior of Hb immobilized in MWCNTs–HA films was studied. As can be seen from Fig. 3A, no redox peaks was observed at MWCNTs–HA/GC (dashed line) in 0.10 M phosphate buffer solution of pH 7.0 at a scan rate of 100 mV s^{-1}, but a pair of well-defined redox peaks were observed at the Hb/MWCNTs–HA/GC (solid line) with the potentials as $E_{pc} = -0.37$ V and $E_{pa} = -0.30$ V (vs. SCE), and the peak-to-peak separation (ΔE_p) was 70 mV

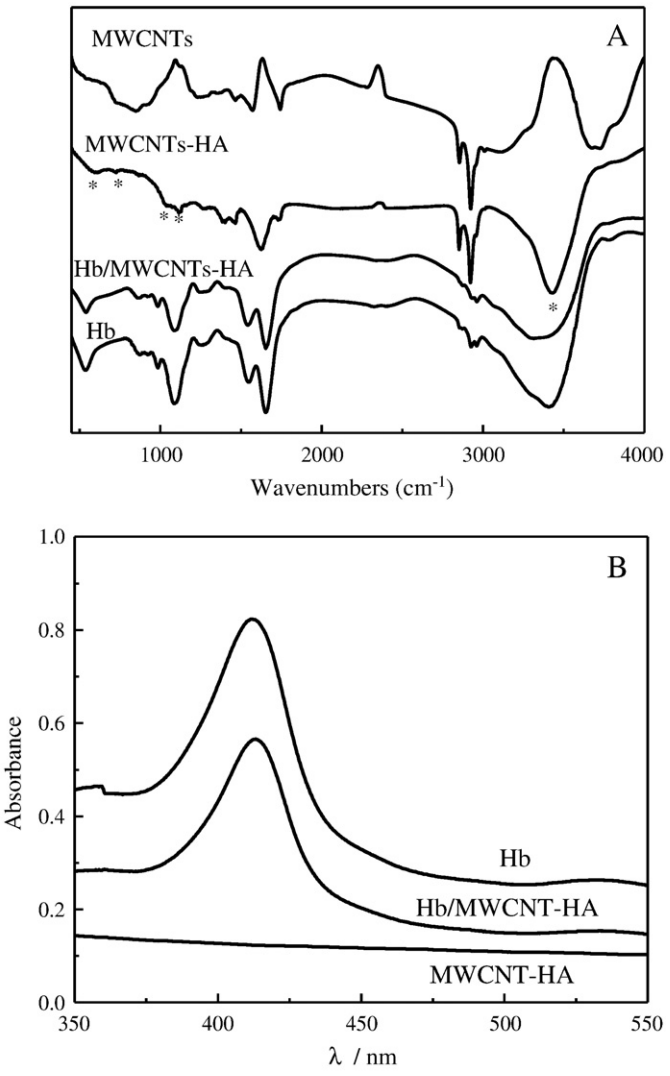

Fig. 2. (A) FT-IR spectra of MWCNTs, MWCNTs–HA, Hb and Hb/MWCNTs–HA. (B) UV–visible spectra of the MWCNTs–HA, Hb and Hb/MWNTs–HA films on indium tin oxide side.

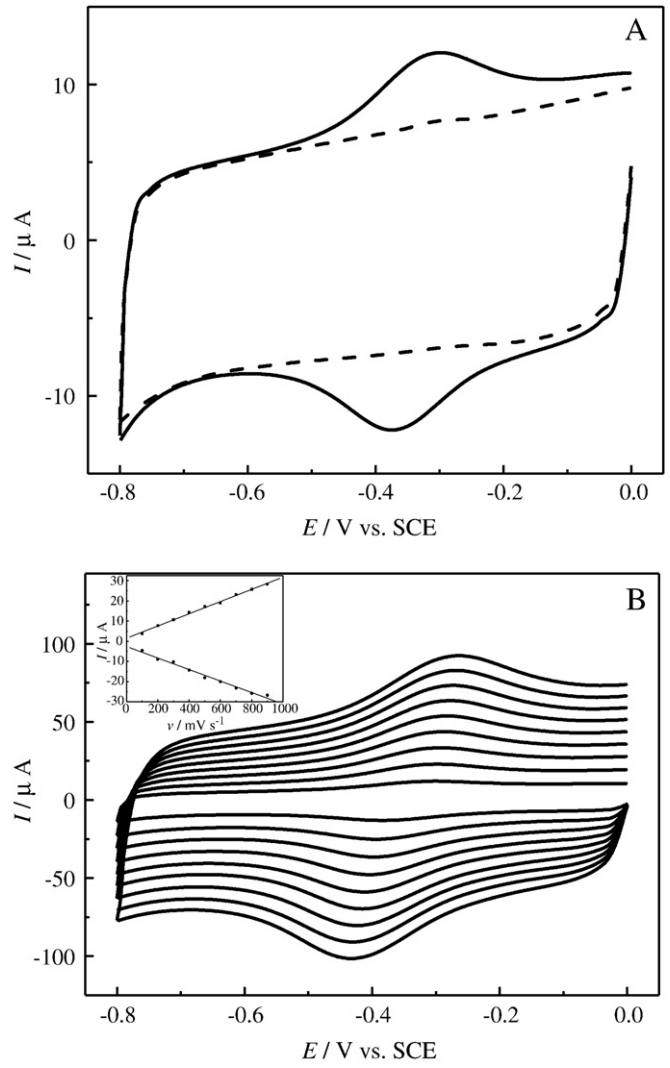

Fig. 3. (A) Cyclic voltammograms (CVs) obtained at MWCNTs–HA/GC (dashed line) and Hb/MWCNTs–HA/GC (solid line) electrodes in 0.10 M N_2-saturated phosphate buffer. (B) CVs obtained at Hb/MWCNTs–HA/GC electrode in 0.10 M N_2-saturated phosphate buffer at 100, 200, 300, 400, 500, 600, 700, 800 and 900 mV s^{-1} (from inner to outer). Inset showed a plot of cathodic and anodic peak currents against potential scan rate.

at the scan rate 100 mV s^{-1}. The formal potential $E^{0'}$, estimated as the average of the anodic and cathodic peak potentials, was −0.335 V (vs. SCE), which is close to that of Hb on other nanomaterials modified electrode in our previous works [6,7,11]. The results indicated that the direct electron transfer achieved between Hb and electrodes were effectively facilitated by the MWCNTs–HA composite film, resulting from the three-dimensional architecture structure of MWCNTs–HA composite film. Moreover, the MWCNTs–HA composite film could provide the micro-environment for the Hb to maintain its suitable conformation and activity.

Fig. 3B shows the CVs for the redox of Hb entrapped in the MWCNTs–HA/GC modified electrodes at various scan rates in 0.10 M phosphate buffer (pH 7.0). It could be observed that the peak currents (I_p) increased with the increase of the scan rate (ν), at the same time, the cathodic and anodic peak potentials exhibited a small shift and the peak current increased along with the rising of scan rate from 100 mV s^{-1} to 900 mV s^{-1}. As shown in the inset of Fig. 3B, the cathodic and anodic peak currents increased linearly with the scan rate. All these results demonstrated that the reaction was a surface controlled and quasi-reversible process between the Hb and MWCNTs–HA composite film.

The apparent heterogeneous electron transfer rate constant (k_s) could be calculated according to the equation derived Laviron for diffusionless CVs as follows [33]

$$E_{p,c} = E^{0'} + \frac{RT}{\alpha F}\ln\frac{RTk_s}{\alpha F\nu};\ E_{p,a} = E^{0'} - \frac{RT}{(1-\alpha)F}\ln\frac{RTk_s}{(1-\alpha)F\nu}$$

$$\Delta E_p = E_{p,a} - E_{p,c} = \frac{RT}{\alpha(1-\alpha)F}\left[-\ln\frac{RTk_s}{F\nu} + (1-\alpha)\ln\alpha + \alpha\ln(1-\alpha)\right]$$

where ν is the scan rate, α is the electron transfer coefficient which can be calculated according to the slopes of anodic process and cathodic process and the result is 0.46 (given $0.3<\alpha<0.7$ in general), and k_s is the apparent heterogeneous electron transfer rate constants which calculated according to ΔE_p versus ln ν. The value of k_s was calculated to be (5.05 ± 0.41) s^{-1}, which was higher than that of Hb immobilized on a mesoTiO_2-modified electrode (1.9 ± 0.15 s^{-1}) [34], carbon nanotube (1.02 ± 0.05 s^{-1}) [35] and on nanocrystalline tin oxide (0.53 s^{-1}) [36]. The results indicated that MWCNTs–HA composite film enhanced the electron transfer process between Hb and electrodes.

We could calculate the surface coverage (Γ^*) according to the Faraday's law, $Q = nFA\Gamma^*$, at different scan rate. Here F is the Faraday constant, n and A stand for the number of electron transferred and the area of the electrode surface, respectively. Q can be obtained by integrating the cathodic peak of Hb. The surface coverage (Γ^*) of Hb at the Hb/MWCNTs–HA/GC electrodes was estimated to be $(9.25\pm0.69)\times10^{-10}$ mol cm^{-2}.

The electrochemical behavior of Hb/MWCNTs–HA/GC modified electrodes on the pH of the electrolyte solution was given in Fig. 4. As can be seen, the electrochemical behavior has a strong dependence on the pH value, and the potentials of anodic and cathodic would shift negatively along with the increased pH value from 5 to 9 in the phosphate buffers for the Hb/MWCNTs–HA/GC modified electrodes. At the same time, the E_{pa}, E_{pc} and $E^{0'}$ exhibited linear relationship with the pH value in the range of 5.0–9.0 in inset of Fig. 4, with slopes of −36.82 mV pH^{-1}, −38.17 mV pH^{-1} and −37.5 mV pH^{-1}, respectively.

3.4. Electrocatalytic of Hb/MWCNTs–HA composite film to H_2O_2 and the trichloroacetic acid

Hemoglobin can be used to reduce oxygen and hydrogen peroxide through electrochemical catalysis based on its intrinsic peroxidase

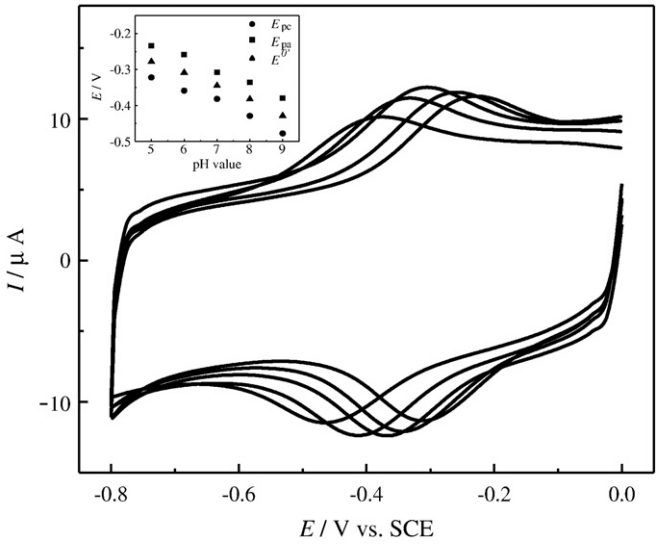

Fig. 4. CVs of Hb/MWCNTs–HA/GC electrode at different pH values. Inset showed the effect of pH value on E_{pa} (■), E_{pc} (●) and $E^{0'}$ (▲) of Hb/MWCNTs–HA/GC electrode in 0.10 M phosphate buffer.

activity. As can be seen from Fig. 5A, the reduction peak at about −0.38 V increased, accompanied with a decrease and disappearance of the oxidation peak for the Hb-immobilized MWCNTs–HA/GC electrodes (dashed line) after adding H_2O_2 into phosphate buffer. On the other hand, the cathodic current peaks gradually increased with the increasing concentration of H_2O_2. The results indicated a typical electrocatalytic activity toward the reduction of H_2O_2.

Fig. 5B exhibits the amperometric response of the Hb/MWCNTs–HA/GC modified electrodes upon the successive additions of H_2O_2 to 0.10 M pH 7.0 PBS at an applied potential of −0.38 V. Obviously, the electrocatalytic current of the biosensor were observed after each addition of H_2O_2 to the solution. The linear range of this biosensor to H_2O_2 concentration was between 0.5–2 μM, which could be described by a linear regression equation of $\Delta I/nA = -0.305 + 3.965$ °C/μM, with the correlation coefficient of 0.999. The detection limit of the biosensor was 0.09 μM based on a signal-to-noise ratio of 3. The results indicated that Hb entrapped in the MWCNT–HA film possessed electrocatalytic activity to H_2O_2. The stability of biosensor was investigated through storing the modified electrodes in a 0.10 M phosphate buffer for 3 weeks at 4 °C. The H_2O_2 biosensor exhibited a good long-term stability and the current decreased 10%.

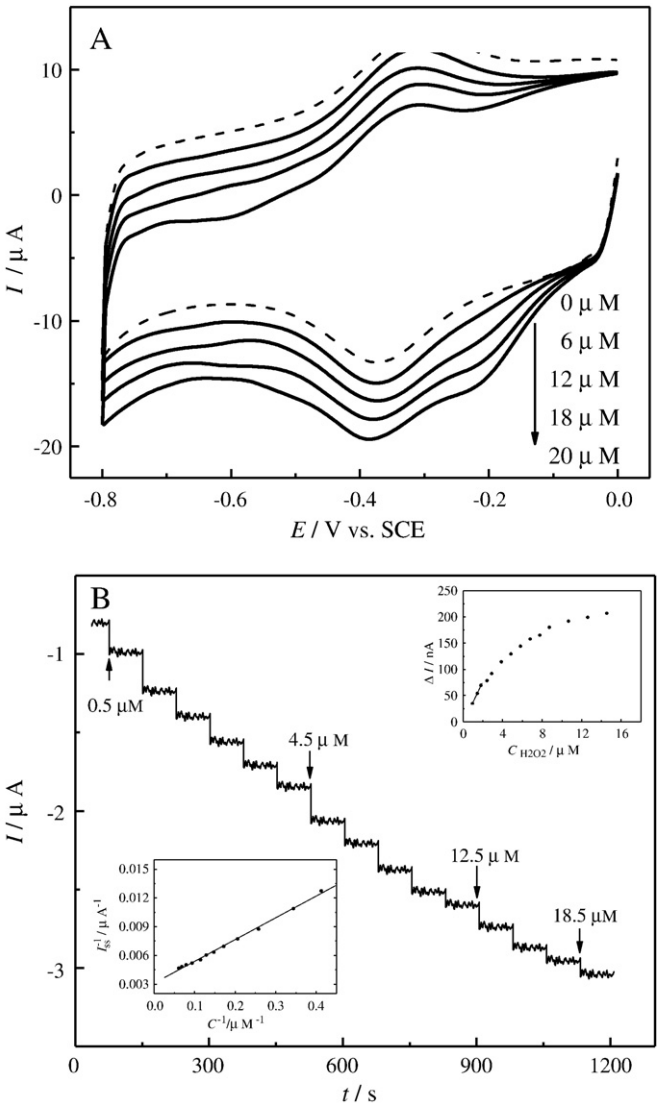

Fig. 5. (A) CVs of Hb/MWCNTs–HA/GC electrode in 0.10 M pH 7.0 phosphate buffer containing different contents of H_2O_2. (B) Amperometric responses of Hb/MWCNTs–HA/GC electrode in stirred solutions to the successive additions of H_2O_2. Insets are the calibration curve (top right) and corresponding Lineweaver–Burk plot (left side).

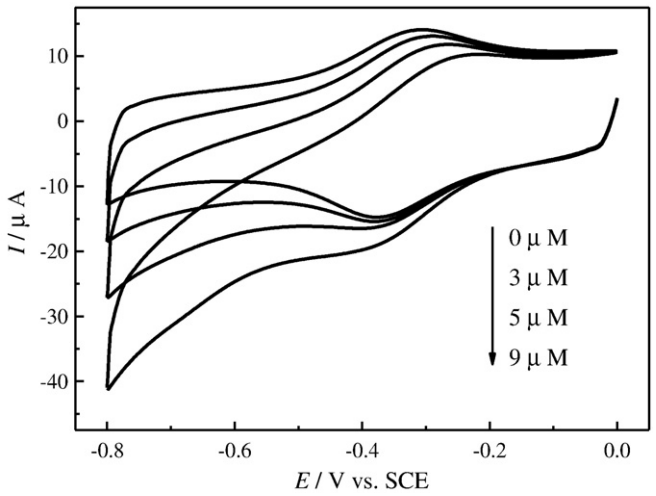

Fig. 6. CVs of Hb/MWCNTs–HA/GC electrode in 0.10 M pH 7.0 phosphate buffer containing different contents of TCA.

A plateau was observed when the concentration of H_2O_2 was higher than 2 μM (top right inset in Fig. 5B). According to the Lineweaver–Burk form of the Michaelis–Menten equation [37]: $1/I_{ss} = (1/I_{max}) + (K_m^{app}/I_{max}c)$. Here I_{ss} is the steady-state current after the addition of a substrate and obtained from amperometric experiments, I_{max} is the maximum current under saturated substrate condition, c is the concentration of the substrate, and K_m^{app} is the apparent Michaelis–Menten constant and is independent of the enzyme concentration. As well known, when the K_m^{app} goes down, the catalytic activity of the immobilized enzyme goes up. The K_m^{app} calculated from the left insert in the Fig. 5B was 7.339 μM. It was markedly smaller than the value in the previous reports [7,12,38]. The result proved that the Hb immobilized in MWCNTs–HA composite film had a higher biological affinity to H_2O_2.

As can be seen from Fig. 6, no redox peaks were observed at the MWCNTs–HA/GC in a 0.10 M phosphate buffer containing TCA (data not shown). When TCA was added into the phosphate buffer gradually, the cathodic current for the Hb-immobilized MWCNTs–HA/GC increased, accompanying with a decrease of anodic current. The results indicated that the Hb-immobilized MWCNTs–HA/GC exhibited the excellent catalytic reactivity toward TCA.

4. Conclusions

We demonstrated that the MWCNTs–HA nanocomposite could provide favorable micro-environment for Hb due to the assembled HA. The direct electron transfer between the immobilized redox proteins in MWCNTs–HA nanocomposite film and the electrode was easily performed. Moreover, the hydrogen peroxide biosensor based on Hb immobilized in MWCNTs–HA nanocomposite film showed a fast amperometric response, very high sensitivity, good reproducibility and stability. In addition, the entrapped Hb showed a good bioelectrocatalytic activity for electrochemical reduction of TCA. These properties were believed to be very useful in the field of bioelectronic nanodevices, e.g., electrochemical biosensor and enzyme-based biofuel cells.

Acknowledgements

This work was supported by the National Natural Science Foundation of China (No. 20805010).

References

[1] D.E. Reed, F.M. Hawkridge, Direct electron transfer reactions of cytochrome *c* at silver electrodes, Anal. Chem. 59 (1987) 2334–2339.
[2] J. Ye, R.P. Baldwin, Catalytic reduction of myoglobin and hemoglobin at chemically modified electrodes containing methylene blue, Anal. Chem. 60 (1988) 2263–2268.

[3] J.F. Rusling, Enzyme bioelectrochemistry in cast biomembrane-like films, Acc. Chem. Res. 31 (1998) 363–369.
[4] L. Gorton, A. Lindgren, T. Larsson, F.D. Munteanu, T. Ruzgas, I. Gazaryan, Direct electron transfer between heme-containing enzymes and electrodes as basis for third generation biosensors, Anal. Chim. Acta 400 (1999) 91–108.
[5] S. Ding, M. Xu, G. Zhao, X. Wei, Direct electrochemical response of myoglobin using a room temperature ionic liquid, 1-(2-hydroxyethyl)-3-methyl imidazolium tetrafluoroborate, as supporting electrolyte, Electrochem. Commun. 9 (2007) 216–220.
[6] W. Zheng, Y.F. Zheng, K.W. Jin, N. Wang, Direct electrochemistry and electrocatalysis of hemoglobin immobilized in TiO_2 nanotube films, Talanta 74 (2008) 1414–1419.
[7] H.Y. Zhao, W. Zheng, Z.X. Meng, H.M. Zhou, X.X. Xu, Z. Li, Y.F. Zheng, Bioelectrochemistry of hemoglobin immobilized on a sodium alginate-multi wall carbon nanotubes composite film, Biosens. Bioelectron. 24 (2009) 2352–2357.
[8] I. Taniguchi, K. Watanabe, M. Tominaga, F.M. Hawkridge, Direct electron transfer of horse heart myoglobin at an indium oxide electrode, J. Electroanal. Chem. 333 (1992) 331–338.
[9] S.F. Wang, T. Chen, Z.L. Zhang, X.C. Shen, Z.X. Lu, D.W. Pang, K.Y. Wong, Direct electrochemistry and electrocatalysis of heme proteins entrapped in agarose hydrogel films in room-temperature ionic liquids, Langmuir 21 (2005) 9260–9266.
[10] L. Gao, Q. Gao, Hemoglobin niobate composite based biosensor for efficient determination of hydrogen peroxide in a broad pH range, Biosens. Bioelectron. 22 (2007) 1454–1460.
[11] W. Zheng, Y.F. Zheng, Gelatin-functionalized carbon nanotubes for the bioelectrochemistry of hemoglobin, Electrochem. Commun. 9 (2007) 1619–1623.
[12] W. Zheng, J. Li, Y.F. Zheng, An amperometic biosensor based on hemoglobin immobilized in poly(ε-caprolactone) film and its application, Biosens. Bioelectron. 23 (2008) 1562–1566.
[13] Y. Yan, W. Zheng, M. Zhang, L. Wang, L. Su, L. Mao, Bioelectrochemically functional nanohybrids through co-assembling of proteins and surfactants onto carbon nanotubes: facilitated electron transfer of assembled proteins with enhanced faradic response, Langmuir 21 (2005) 6560–6566.
[14] P. Yu, Y. Lin, L. Xiang, L. Su, J. Zhang, L. Mao, Molecular films of water-miscible ionic liquids formed onto glassy carbon electrode: characterization and electrochemical applications, Langmuir 21 (2005) 9000–9006.
[15] Y. Kong, M. Boopathi, Y. Shim, Direct electrochemistry of horseradish peroxidase bonded on a conducting polymer modified glassy carbon electrode, Biosens. Bioelectron. 19 (2003) 227–232.
[16] B.A. Gregg, A. Heller, Cross-linked redox gels containing glucose oxidase for amperometric biosensor applications, Anal. Chem. 62 (1990) 258–263.
[17] W. Shan, H. Liu, J. Shi, L. Yang, N. Hu, Self-assembly of electroactive layer-by-layer films of heme proteins with anionic surfactant dihexadecyl phosphate, Biophys. Chem. 134 (2008) 101–109.
[18] Y. Hu, H. Sun, N. Hu, Assembly of layer-by-layer films of electroactive hemoglobin and surfactant didodecyldimethylammonium bromide, J. Colloid Interface Sci. 314 (2007) 131–140.
[19] K. Gong, Y. Yan, M. Zhang, S. Xiong, L. Mao, Electrochemistry and electroanalytical applications of carbon nanotubes: a review, Anal. Sci. 21 (2005) 1383–1393.
[20] C.V. Nguyen, L. Delzeit, A.M. Cassell, J. Li, J. Han, M. Meyyappan, Preparation of nucleic acid functionalized carbon nanotube arrays, Nano Lett. 2 (2002) 1079–1081.
[21] C.A. Dyke, J.M. Tour, Solvent-free functionalization of carbon nanotubes, J. Am. Chem. Soc. 125 (2003) 1156–1157.
[22] J.L. Stevens, A.Y. Huang, H. Peng, I.W. Chian, V.N. Khabashesku, J.L. Margrave, Sidewall amino-fuctionalization of single-walled carbon nanotubes through fluorination and subsequent reactions with terminal diamines, Nano Lett. 3 (2003) 331–336.
[23] I. Sopyan, M. Mel, S. Ramesh, K.A. Khalid, Porous hydroxyapatite for artificial bone application, Sci. Technol. Adv. Mater. 8 (2007) 116–123.
[24] F. Mei, J. Zhong, X. Yang, X. Quyang, S. Zhang, X. Hu, Q. Ma, J. Lu, S. Ryu, X. Deng, Improved biological characteristics of poly(L-lactic acid) electrospun membrane by incorporation of multiwalled carbon nanotubes/hydroxyapatite nanoparticles, Biomacromolecules 8 (2007) 3729–3735.
[25] K. Balani, Y. Chen, S.P. Harimkar, N.B. Dahotre, A. Agarwal, Tribological behavior of plasma-sprayed carbon nanotube-reinforced hydroxyapatite coating in physiological solution, Acta Biomater. 3 (2007) 944–951.
[26] S. Liao, G. Xu, W. Wang, F. Watari, F. Cui, S. Ramakrishna, C.K. Chan, Self-assembly of nano-hydroxyapatite on multi-walled carbon nanotubes, Acta Biomater. 3 (2007) 669–675.
[27] L. Feng, H. Li, F. Li, Z. Shi, Z. Gu, Functionalization of carbon nanotubes with amphiphilic molecules and their Langmuir–Blodgett films, Carbon 41 (2003) 2385–2391.
[28] M.K. Kumar, A.L.M. Reddy, S. Ramaprabhu, Exfoliated single-walled carbon nanotube-based hydrogen sensor, Sens. Actuators, B, Chem. 130 (2008) 653–660.
[29] V.M. Bhatnagar, X-ray and infrared studies of lead apatites, Can. J. Chem. 49 (1971) 662–663.
[30] S.R. Bhattarai, S. Aryal, K.C.R. Bahadur, N. Bhatarai, P.H. Hwang, H.K. Yi, H.Y. Kim, Carbon nanotube-hydroxyapatite nanocomposite for DNA complexation, Mater. Sci. Eng., C 28 (2008) 64–69.
[31] J.K. Kauppinen, D.J. Moffate, H.H. Mantsch, D.G. Lameron, Fourier self-deconvolution: a method for resolving intrinsically overlapped bands, Appl. Spectrosc. 35 (1981) 271–276.
[32] H. Theorell, A. Ehrenberg, Spectrophotometric, magnetic and titrimetrie studies on the heme-linked groups in myoglobin, Acta Chem. Scand. 5 (1951) 823–848.
[33] E. Laviron, General expression of the linear potential sweep voltammogram in the case of diffusionless electrochemical systems, J. Electroanal. Chem. 61 (1979) 19–28.
[34] N. Jia, Y. Wen, G. Yang, Q. Lian, C. Xu, H. Shen, Direct electrochemistry and enzymatic activity of hemoglobin immobilized in ordered mesoporous titanium oxide matrix, Electrochem. Commun. 10 (2008) 774–777.
[35] R. Zhang, X. Wang, K. Shiu, Accelerated direct electrochemistry of hemoglobin based on hemoglobin-carbon nanotube (Hb-CNT) assembly, J. Colloid Interface Sci. 316 (2007) 517–522.
[36] E. Topoglidis, Y. Astuti, F. Duriaux, M. Gratzel, J.R. Durrant, Direct electrochemisty and nitric oxide interaction of heme proteins adsorbed on nanocrystalline tin oxide electrodes, Langmuir 19 (2003) 6894–6900.
[37] R.A. Kamin, G.S. Wilson, Rotating ring-disk enzyme electrode for biocatalysis kinetic studies and characterization of the immobilized enzyme layer, Anal. Chem. 52 (1980) 1198–1205.
[38] W. Zheng, J. Li, Y.F. Zheng, Preparation of poly(L-lactide) and its application in bioelectrochemistry, J. Electroanal. Chem. 621 (2008) 69–74.